Behaviour of a Mixture of Coal Wash and Rubber Crumbs under Cyclic Loading

Miriam Tawk[1]; Yujie Qi, Ph.D., AMASCE[2]; Buddhima Indraratna, Ph.D., F. ASCE[3]; Cholachat Rujikiatkamjorn, Ph.D.[4]; Ana Heitor, Ph.D., MIEAust[5]

[1]PhD Candidate, School of Engineering and Information Sciences, University of Wollongong, Wollongong, NSW 2522, Australia. E-mail: mst055@uowmail.edu.au

[2]Lecturer, Transport Research Centre, School of Civil and Environmental Engineering, University of Technology Sydney, Sydney NSW 2007, Australia. E-mail: yujie.qi@uts.edu.au

[3]Distinguished Professor of Civil Engineering, Founding Director of Australian Research Council's Industrial Transformation Training Centre for Advanced Technologies in Rail Track Infrastructure (ITTC-Rail), Director of Transport Research Centre, University of Technology Sydney, Sydney, NSW 2007, Australia. E-mail: buddhima.indraratna@uts.edu.au

[4]Professor, School of Civil and Environmental Engineering, University of Technology Sydney, Sydney 2007, Australia. E-mail: cholachat.rujikiatkamjorn@uts.edu.au

[5]Lecturer, Centre for Cities and Infrastructure and Institute for High Speed Rail and System Integration, School of Civil Engineering, University of Leeds, Leeds, UK. E-mail: a.heitor@leeds.ac.uk

†Author for correspondence:
Prof. Buddhima Indraratna
Director, Transport Research Centre,
University of Technology Sydney
Email: Buddhima.indraratna@uts.edu.au

Accepted by: ASCE Journal of Materials in Civil Engineering

ABSTRACT

The interest in the utilization of granular waste materials as construction fills in lieu of quarried natural aggregates has been increasing recently resulting in more sustainable and cost-effective industry practices being adopted. This study proposes a mixture of coal wash (CW; by-product of coal mining) and rubber crumbs (RC; shredding of waste rubber tyres), as a potential capping composite for railways. A series of cyclic triaxial tests mimicking typical rail traffic loads were conducted on CWRC mixtures with and without rest periods to gain an insightful understanding of the deformation mechanism of rubber particles. It is found that the inclusion of RC increases the axial permanent strain, the volumetric strain and the damping ratio, and reduces the resilient modulus, the shear modulus and the breakage index (BI). Also, it is found that the mixture with RC recovers part of its energy dissipation efficiency after a rest period is applied, reducing the breakage index further even when the number of load cycles increases. Accordingly, a modified equation is proposed to determine the void ratio capturing the deformation of rubber.

Keywords: Coal wash; Rubber crumbs; Cyclic loading; Dynamic properties; Energy dissipation.

INTRODUCTION

The reuse of waste materials in transportation infrastructure has been the subject of numerous studies in the past decade. Such initiatives emerge as a result of the strict environmental restrictions applied to the provision of raw quarried aggregates for construction activities. Coal wash (CW), a waste produced by the coal mining industry, and rubber crumbs (RC) shredded form waste tyres, are example waste materials that can be used as construction fills. However, the proactive use of these marginal materials has been limited due to the lack of extensive experimental and field data to provide confidence to transport authorities to replace traditional aggregates with such waste mixtures. For instance, only 7.9% of the scrap tyre derivatives was used in civil engineering projects in the USA in 2017 (U.S. Tire Manufacturers Association 2018). Moreover, the wide variation of properties of CW from one source to another, and the current lack of technical standards for using them influence the decisions to reject them. Nonetheless, in recent years, numerous studies have proposed CW as a potential construction fill and investigated its geotechnical properties (e.g. Heitor et al. 2016; Indraratna 1994; Leventhal 1996; Leventhal and De Ambrosis 1985; Montgomery 1990; Okagbue and Ochulor 2007; Rujikiatkamjorn et al. 2013; Chiaro et al. 2015; Tasalloti et al. 2015; Wang et al. 2019; Indraratna et al. 2020). More recently, Indraratna et al. (2018) optimized a mixture of CW, RC and steel furnace slag (SFS) to minimize particle degradation and improve its energy absorption and damping properties and the dynamic properties of the mixture as appropriate for heavy haul tracks were also investigated by Qi et al. (2018ab) and Qi and Indraratna (2020).

Due to the lightweight and energy absorbing nature of rubber, numerous research initiatives have considered to use the recycled rubber by mixing it with other traditional aggregates such as sand and gravel (e.g. Ahmed 1993; Feng and Sutter 2000; Lee et al. 1999; Senetakis et al. 2012; Signes et al. 2016; Youwai and Bergado 2003) and with other waste materials such as

77 recycled glass (Saberian et al. 2019) and recycled concrete (Saberian et al. 2018). While most
78 of these studies have mainly focused on the effect of rubber on shear strength, axial and
79 volumetric strain and strain energy dissipation under static loading conditions, very limited
80 research have properly evaluated the behaviour of rubber-aggregate mixtures using cyclic
81 triaxial tests (e.g. Qi et al. 2018b) to simulate dynamic live loads in transport corridors. When
82 the dynamic response of rubber-aggregate mixtures was considered in a few studies, only the
83 small strain behaviour was examined through resonant column tests or shaking table tests
84 (e.g. Feng and Sutter 2000; Senetakis et al. 2012). Also, to the authors' knowledge no
85 previous studies have accurately investigated the deformation characteristics capturing the
86 rebound effect of compressed rubber, which can only be understood better by introducing a
87 rest period between the load cycles. In a track, the substructure is not subjected to dynamic
88 loads continuously, i.e. rest periods simulate the time intervals between a given number of
89 cycles (trains) which reflects more realistic field conditions. Moreover, previous studies of
90 the authors, e.g. Indraratna et al. (2019ab; 2020) have evaluated the compaction
91 characteristics and the stress-strain behaviour of the mixture of CW and RC (CWRC) under
92 the static loading condition. As the CWRC mixture is intended for use as a capping material
93 in lieu of traditional quarried aggregates for railway infrastructure, it is imperative to
94 investigate its geotechnical characteristics under dynamic loading.
95 In this paper, a series of drained cyclic triaxial tests was carried out on CWRC mixtures with
96 different RC contents to investigate the role of rubber inclusion on their geotechnical
97 properties under cyclic loads (i.e. deformation behaviour, the resilient modulus, the damping
98 properties and the breakage index). Also, the effect of a resting period between the cyclic
99 loads on the resilient behaviour was examined with a focus on the recoverable strain before
100 and after the rest period. Local strain measurement was used to capture the deformation of
101 rubber particles and to differentiate between the total volumetric strain and the void

volumetric strain. Accordingly, a new equation was derived to determine the void ratio considering the change in the volume of the solid phase.

MATERIALS AND TESTING PROGRAM

Coal wash (CW) and rubber crumbs (RC) were procured from a colliery north of Wollongong City, and a tyre recycling company near Melbourne, respectively. CW was a well-graded material with a specific gravity of 2.25 and the rubber crumbs were relatively angular with a much smaller specific gravity of 1.15. Four CWRC mixtures with 0%, 5%, 10% and 15% RC (by weight) were considered in this study. The range of rubber contents was selected based on a previous study by Indraratna et al. (2018) which found that the optimum rubber content in a mixture of CW, RC and steel furnace slag is around 10%. Higher rubber contents would significantly reduce the strength of the mixture, i.e. make it overly compressible and vulnerable to deformation (settlement) (Qi and Indraratna 2020). The particle size distribution (PSD) curves of CW, RC and the CWRC mixtures as well as the upper and lower PSD limits for capping materials specified by the Australian Rail Track Corporation (ARTC, 2010) are shown in Fig.1. Coal wash was sieved and separated into different size ranges and the exact weight of each size category was obtained according to the target PSD curves, in order to prepare triaxial specimens of 100 mm in diameter having a height of 200 mm. Rubber crumbs were added at different weight proportions and the mixture was thoroughly mixed. Water was then added to reach the target moisture content (≈ 9-10 %) and the mixture was left in a sealed container under constant temperature and humidity to ensure a consistent water equilibration (Indraratna et al. 2019b).

The triaxial test specimens were then prepared by compacting the mixture in 5 layers, where each layer was compacted until the required thickness to achieve the target void ratio (≈0.29) was attained. The target void ratio was determined by considering the dry density specification of the Australian Rail Track Corporation (ARTC, 2010) as explained by

Indraratna et al. (2019b). In total, 16 cyclic triaxial tests were performed on four CWRC mixtures. At the outset, 12 tests were performed to study the effect of the cyclic stress ratio (CSR) and the confining pressure on the axial strain, volumetric strain, resilient modulus and damping properties of CWRC mixtures. Then, another series of 4 cyclic triaxial tests was performed under an effective confining pressure (σ_3') of 25 kPa and a cyclic deviator stress (q_{cyc}) of 100 kPa, typical conditions for a subballast/capping layer (Signes et al. 2016), where a rest period was introduced every 40,000 cycles for a duration of 10 minutes, and the sample was subjected to a total of 480,000 cycles. The duration of the rest period was selected to reflect the average time between the passages of two consecutive trains in peak times. For this series of tests, *Hall Effect* sensors were used to measure the radial deformation in the middle of the sample (Fig. 2) and to accurately determine the total volumetric strain. The details of all cyclic triaxial tests are listed in Table 1.

Before starting with the cyclic loading tests presented in this manuscript, a few dummy tests were performed to calibrate the GDS system and select the appropriate stiffness index. Also, parallel samples were tested under a confining pressure of 25 kPa and a cyclic deviator stress of 100 kPa (CSR = 2.0) and this variation was found to be less than 2.5%. The cyclic triaxial tests were performed in three stages, namely saturation, consolidation and dynamic loading. During saturation, the back pressure was increased gradually at a rate of 1 kPa/min until a Skempton B-value greater than 0.97 was reached. Then, the sample was consolidated under the target σ_3' until ignorable volume change (< 5 mm^3) was recorded within 5 minutes. Finally, cyclic loading was applied under drained conditions and a frequency of 10 Hz and different loading conditions as listed in Table 1. In dynamic testing, the CSR is usually used to relate the maximum deviator stress, q_{cyc}, and σ_3':

$$CSR = \frac{q_{cyc}}{2\sigma_3'} \quad (1)$$

In this study, two other ratios, namely YCSR and PCSR (Eqs. 2 and 3), are introduced to relate the maximum cyclic deviator stress, q_{cyc}, with the monotonic yield deviator stress, q_{yield}, and the monotonic peak deviator stress, q_{peak}, respectively (Lackenby et al. 2007; Suiker et al. 2005), and they defined as:

$$YCSR = \frac{q_{cyc}}{q_{yield}} \tag{2}$$

$$PCSR = \frac{q_{cyc}}{q_{peak}} \tag{3}$$

In a monotonic triaxial test, q_{yield} corresponds to the deviator stress at the characteristic state (the phase transformation state under undrained conditions) at which the behaviour of the material shifts from contractive to dilative. The q_{peak} is the maximum deviator stress determined from the stress-strain curve. The values of q_{yield} and q_{peak} were determined from a previous study on the CWRC mixture of the authors (Indraratna et al. 2019b).

EXPERIMENTAL RESULTS

Axial Strain

Figure 3(a-c) shows the permanent axial strain of the CWRC mixtures with 0%, 5%, 10% and 15% RC considering different values of CSR and confining pressure for up to 200,000 cycles. For all the stress conditions, the axial strain increases with increasing rubber contents, and this is an expected outcome associated with the deformation and compression of rubber particles. For the same CSR, there is a slight increase in the permanent axial strain when the deviator stress and the confining pressure increase simultaneously. For instance for the mixture with RC = 15%, the permanent axial strain after 200,000 cycles increases from 1.4% to 2.1%. However, the axial strain increases significantly when the CSR increases to 2.0 with a confining pressure of 25 kPa and a deviator stress of 100 kPa, and the rise is more evident for the mixtures with rubber. It is also noted that the major increase in axial strain occurs

171 when the mixture has 5% added rubber, and the axial strain increases at a slower rate for the
172 mixtures with higher rubber contents (i.e. 10% and 15%). For instance, in the specimen with
173 RC = 5%, RC = 10% and RC = 15%, an increase of 360%, 255% 192%, respectively, is
174 measured when the CSR increases to 2.0 with a confining pressure of 25 kPa.
175 During cyclic loading, cyclic densification is defined as the gradual accumulation of the
176 plastic axial strain with every load cycle. When the growth of plastic strain reaches a plateau,
177 the material is then considered to have reached a state of shakedown, where the loading-
178 unloading curve becomes purely elastic with no further accumulation of plastic strain (Lekarp
179 et al. 2000b). Nonetheless, if the cyclic axial stress is greater than a threshold stress described
180 as the "critical shakedown limit", the material would exhibit an incremental failure
181 accompanied with a progressive accumulation of plastic strain. It has been reported that the
182 ratio between the "critical shakedown limit" (which separates the stable conditions from the
183 incremental failure conditions) and the failure stress under monotonic loading conditions (i.e.
184 critical PCSR) ranges between 0.58 and 0.98 for gravel and crushed stone (Lekarp et al.
185 2000b). As the definition implies, shakedown is better investigated over a range of load
186 cycles, rather than the incremental strain over one cycle. Accordingly, the incremental
187 permanent axial strain over different ranges of load cycles is illustrated in Fig. 3(d-e).
188 Different shakedown criteria have been proposed in the literature based on the incremental
189 strain for a given number of load cycles. For instance, according to Werkmeister et al. (2001)
190 and Gu et al. (2017), unbound granular materials are considered to reach shakedown if the
191 incremental plastic strain between the 3000^{th} and 5000^{th} cycle is less than 0.045% and 0.06%,
192 respectively. Otherwise, incremental collapse is expected to occur after a large number of
193 cycles with a significant build-up of the permanent axial strain. However, this criterion can
194 only be applied to rigid aggregates where shakedown is expected to happen during the first
195 few load cycles.

It is clear from Fig. 3 that for the mixture with no rubber, shakedown is attained after only a few cycles (100 cycles), as the incremental strain over the subsequent 900 cycles is less than 0.03%. For 5% rubber content, plastic shakedown is attained after 1,000 cycles knowing that the incremental plastic strain becomes less than 0.2% between 1,000 and 10,000 cycles, which is equivalent to 0.04% over 2000 cycles. When more than 5% of RC is added to the mixture, shakedown is still attained, but only after a larger number of cycles (10,000 cycles), where a total incremental strain of less than 0.15% is recorded for the next 90,000 cycles (i.e. 0.003% over 2000 cycles). If the loading-unloading curve becomes a straight line, the phenomenon is called "elastic shakedown". Otherwise, if the residual stress-strain response is a closed-loop, the final steady state is depicted as "plastic shakedown" (Collins et al. 1993). It is noteworthy that the material exhibits a "plastic shakedown" as illustrated in Fig. 4 which shows that the residual stress-strain response after 200,000 cycles is a closed-loop rather than a purely elastic straight line. These results indicate that despite the reduction in its strength when rubber is added to the mixture, the inclusion of rubber does not prevent shakedown. It only results in longer periods of cyclic densification before plastic shakedown is attained. Also, incremental collapse is not observed for all mixtures even when an axial stress around the yield stress (YCSR = 1.0) and a PCSR as high as 0.76 are applied.

Figure 5a shows the permanent axial strain for CWRC mixtures tested under a confining pressure of 25 kPa and a cyclic deviator stress of 100 kPa with rest periods. For the mixture with no rubber, the permanent axial strain is almost constant before and after each rest period. When rubber is added, the permanent axial strain decreases during the rest period and increases back to the same level after each rest period, and the reduction becomes more evident when rubber content increases. This indicates that during the cyclic loading, energy is being stored in the sample through the accumulation of a resilient strain. Figure 5(b-e) shows the resilient strain (ε_1^r) before and during the rest period. The resilient strain ε_1^r is the

difference between the maximum axial strain, $\varepsilon_{1,max}$ and the minimum axial strain, $\varepsilon_{1,min}$ during one loading cycle:

$$\varepsilon_1^r = \varepsilon_{1,max} - \varepsilon_{1,min} \quad (4)$$

It is observed that the resilient strain measured during cyclic loading (i.e. before applying the rest period) increases only slightly when rubber content increases; this is attributed to the high frequency used in this study (i.e. 10 Hz), where the mixture cannot fully recover its elastic strain before the next load cycle is applied. On the other hand, the resilient strain after the rest period increases significantly with increasing rubber content. This indicates that when a rest period is introduced and the load is completely removed, the energy cumulatively stored through the compression of rubber particles is released through a partial rebound of RC resulting in a further increase in the resilient strain.

Volumetric strain

Assuming fully drained conditions for granular materials, the permanent void volumetric strain, ε_v^*, measured by controlling the volume of water inside the sample, V_w (under drained saturated conditions) represents only the change in the volume of voids, V_v, as expressed in the equation below:

$$\varepsilon_v^* = \frac{\Delta V_v}{V_0} = \frac{\Delta V_w}{V_0} \quad (5)$$

The void volumetric strain of CWRC mixtures measured using the water controller under different stress conditions is shown in Fig. 6(a-c). A contractive behaviour is observed for the entire duration of cyclic loading (200,000 cycles) for all the mixtures and all stress conditions considered herein, even for YCSR = 1.0. It is noteworthy that YCSR of 1.0 means that the cyclic stress is equal to the yield stress which separates the contractive behaviour from the dilative behaviour under monotonic loading conditions. The rate of accumulation and the value of the volumetric strain increase as the rubber content increases from 0% to 15%. This

is more evident in Fig. 6(c) when a confining pressure of 25 kPa and a cyclic deviator stress of 100 kPa are applied, and this is attributed to the compressible nature of RC which facilitates the sliding and rearrangement of particles into a more compact packing.

To measure the total volumetric strain (ε_v) which accounts for both the change in the volume of voids and rubber particles, the hall effect sensors were used to measure the radial strain (see Fig. 2). Then, the total volumetric strain was calculated using the following equation:

$$\varepsilon_v = \frac{\Delta V}{V_0} = \frac{\Delta(V_v + V_{RC})}{V_0} = \varepsilon_1 + 2\varepsilon_3 \quad (6)$$

where V_{RC} is the volume of RC and V_0 is the initial volume of the sample, ε_1 is the axial strain and ε_3 is the radial strain. Figure 7a shows the void volumetric strain, ε_v^*, and the total volumetric strain, ε_v, for all CWRC mixtures under a confining pressure of 25 kPa and a cyclic deviator stress of 100 kPa. It is noteworthy that rebound behaviour is observed for the total and void volumetric strain when a rest period is applied. For the mixture with no RC, the difference between the void volumetric strain and the total volumetric strain is negligible. For all the mixtures with RC, there is a difference between the void volumetric strain, ε_v^*, and the total volumetric strain, ε_v and it is evident that the difference is more pronounced at higher rubber contents. This reflects the change in the volume of solids (i.e. RC) within the mixture, V_s, which is not accounted for in the void volumetric strain. For a granular assembly with a compressible component, a solid volumetric strain, ε_v^s, can be defined as:

$$\varepsilon_v^s = \frac{\Delta V_s}{V_0} = \varepsilon_v - \varepsilon_v^* \quad (7)$$

Figure 7b shows the effect of rubber content and the rest period on the solid volumetric strain of the CWRC mixtures. It is noted that the mixture with no rubber shows no volume change in its solid phase under cyclic loading. As a result of rubber compression and deformation the solid volumetric strain due to rubber increases significantly when 5% RC is added to the mixture with a lesser increase when more rubber is added (i.e. 10% and 15%). Like the void

volumetric strain, a dilative behaviour is observed after each rest period. This indicates that when the test is stopped and the load is completely removed, rubber particles attempt to partially recover their original volume resulting in a dilative behaviour. Nevertheless, the initial volume cannot be fully recovered due the internal confinement by surrounding rigid particles (i.e. CW) created during cyclic densification.

Void ratio

In traditional soil mechanics, the volume of solids is assumed to be constant and the change in the void ratio is determined as:

$$\Delta e = \frac{\Delta V_v}{V_s} \tag{8}$$

where, e is the void ratio, V_v is the volume of voids and V_s is the volume of the solid phase. Accordingly, the relationship between the void ratio and the void volumetric strain is expressed as:

$$e = e_0 + \varepsilon_v^*(1 + e_0) \tag{9}$$

where, e_0 is the initial void ratio and ε_v^* is the void volumetric strain. While this equation is applicable to conventional rigid aggregates like sand and gravel, the volume of solids cannot be assumed to be a constant when a compressible component like rubber is added to the mixture (Fig. 7b). An alternative equation that considers the change in the volume of solids is then derived as (Tawk et al. 2020):

$$e = \frac{\left(\frac{e_0}{1 + e_0}\right) + \varepsilon_v^*}{(1 + \varepsilon_v) - \left[\left(\frac{e_0}{1 + e_0}\right) + \varepsilon_v^*\right]} \tag{10}$$

When the solids within the mixture are not compressible and ($\varepsilon_v^* = \varepsilon_v$), Eq. 10 reverts to the original equation (i.e. Eq. 9). Figure 8 shows the void ratio calculated using both Eq. 9 and Eq. 10. For the mixture with no rubber, the difference between the values calculated using Eq. 9 and Eq. 10 is insignificant given that the change in the volume of solids (i.e. CW

particles) is minor, hence both equations would yield the same result. Nevertheless, when rubber is added to the mixture, the void ratio calculated using Eq. 10, which considers the change in the volume of RC, is smaller than the void ratio determined from the classical equation (Eq. 9). Also, during the first 100 cycles, the void ratio of the mixtures with added rubber increases even though a compressive behaviour is observed from the void volumetric strain. This is associated with a simultaneous reduction in the volume of solids resulting in an initial increase in the void ratio. The above observations indicate that classical soil mechanics relationships that were initially developed for relatively incompressible and rigid granular materials cannot be directly extrapolated to describe the behaviour of mixtures with a compressible component like RC.

Resilient Modulus, Shear Modulus and Damping ratio

The resilient modulus is defined as the ratio of the difference between the maximum and the minimum cyclic deviator stress, Δq_{cyc}, and the recoverable strain, ε_1^r, during a load cycle, and is typically measured when a state of elastic or plastic shakedown is attained :

$$M_r = \frac{\Delta q_{cyc}}{\varepsilon_1^r} \tag{11}$$

Figure 9 shows the relationship between the resilient modulus and the number of cycles for CWRC mixtures under different stress conditions. In general, the resilient modulus decreases with increasing rubber contents, a behaviour resulting from the increased elasticity by adding rubber. M_r of CWRC mixtures with RC $\geq$ 10% reaches a stable state after 10,000 loading cycles, while a fewer number of cycles is needed to reach a stable condition for 0% and 5% RC. When tested at a constant CSR of 0.8, M_r increases when σ'_3 and q_{cyc} increase. Moreover, when the CSR increases from 0.8 to 2.0 under an effective confining pressure $\sigma'_3 = 25$ kPa (i.e. q_{cyc} increases from 40 kPa to 100 kPa), M_r also increases (Fig. 9a and 9c). However, when the CSR increases from 0.8 to 2.0 but σ'_3 decreases from 50 kPa to 25 kPa,

M_r decreases (Fig. 8b and 8c) despite the increase in q_{cyc}. This indicates that the resilient modulus of the CWRC mixture is more affected by the confining pressure than the CSR, and the effect of the CSR is better investigated if the confining pressure is kept constant.

The damping ratio (D) is an important parameter in soil dynamics as it represents the efficiency of energy dissipation in the system during a load cycle. The higher the damping ratio, the more efficiently the system can dissipate energy. The damping ratio is calculated as the area enclosed within the loop formed in the stress-strain space during one load cycle divided by the area of the triangle representing full energy recovery (linear elastic response) as shown in Fig. 10a. The shear modulus, G, is a parameter related to the stiffness of the material and is determined in the shear stress-shear strain plane (Fig. 10a). Figure 10b shows that the damping ratio of the CWRC mixture increases with the increasing rubber content. For the same CSR, when σ'_3 increases from 25 to 50 kPa and the cyclic deviator stress, q_{cyc} increases from 40 to 80 kPa, the damping ratio remains constant for all CWRC mixtures. However, when the CSR increases from 0.8 to 2.0 the damping ratio of the mixture without rubber decreases significantly, while the mixtures with rubber maintain somewhat the same damping ratio. This indicates that the damping ratio of rigid materials (CW) is dependent on the CSR regardless of the confining pressure and the cyclic deviator stress. This indicates that, an increase in CSR reduces the efficiency of the CW to dissipate energy due to high levels of cyclic densification. When rubber is added, the rubber particles sustain the energy dissipation efficiency of the mixture through compression and deformation even after undergoing cyclic densification under higher values of CSR.

The shear modulus vs. rubber content is shown in Fig. 11 for all stress conditions. Generally, the shear modulus decreases with increasing rubber contents. Similarly, this is attributed to the elasticity of rubber which contributes to the overall reduction in the stiffness of the mixture. Under the same CSR, the shear modulus increases when both the confining pressure

and the cyclic deviator stress increase, but the variation becomes less evident as the rubber content increases. A similar behaviour was reported by Qi et al. (2018b) for the mixtures of CW, RC and SFS when tested under three stress conditions with the same CSR. In contrast, when the confining pressure remains constant at 25 kPa and the CSR increases from 0.8 (q_{cyc} = 40 kPa) to 2.0 (q_{cyc} = 100 kPa), the shear modulus remains almost constant. This indicates that, similar to the resilient modulus, the shear modulus of the CWRC mixtures is highly dependent on the confining pressure, while the cyclic deviator stress does not show a significant effect when the same confining pressure is applied.

Breakage Index and Energy Dissipation

CW is a weak material with a very high potential for breakage. Blending CW with an energy absorbing material like rubber could mitigate the degradation of CW particles when subjected to repeated loads. Breakage of the CWRC mixture after cyclic loading was evaluated using the Breakage Index (BI) proposed by Indraratna et al. (2005) and Fig. 12 shows the BI of the mixtures under an effective confining pressure of 25 kPa and a cyclic deviator stress of 100 kPa with and without a rest period. As expected, it is observed that the BI decreases with increasing rubber contents. For the mixture with RC $\leq$ 5%, the BI evaluated after 480,000 cycles when a rest period was applied every 40,000 cycles is greater than the BI determined after 200,000 cycles with no rest period. This is an expected outcome since the mixture is subjected to a higher number of load cycles. Nevertheless, for the mixture with RC $\geq$ 10%, the BI evaluated after 200,000 cycles with no rest period is greater than the BI evaluated after 480,000 cycles with a rest period even though the number of cycles is almost doubled for the latter case.

To further explore the effect of having a rest period, the corresponding stress-strain loop is illustrated in Fig. 13a. After a sufficient number of cycles, the mixture reaches plastic shakedown and the stress-strain loop becomes fully resilient (Fig. 13a 1-2 states) (i.e. no

358 further accumulation of plastic strain). When there is a rest period and the external vertical
359 load is completely removed, the recoverable strain, ε_1^r, increases further due to the rebound of
360 rubber particles (Fig 13a 2-3 states). When the load is applied again, the mixture goes
361 through another cyclic densification stage (Fig 13a 4-5-6 states) before reaching plastic
362 shakedown again (Fig 13a 2-1-2 states). It is evident form Fig. 13b that the total energy
363 dissipated during the first cycle after the rest period is much higher than the energy dissipated
364 during the last cycle before the rest period, i.e. when the mixture reached shakedown.
365 An efficiency ratio (ER) can be defined as the ratio between the total input energy and the
366 total energy dissipated during one load cycle:

$$ER = \frac{E_{dis}}{E_{total}} = \frac{E_{total} - E_{res}}{E_{total}} \tag{12}$$

367 where

$$E_{total} = \int_{\varepsilon_{min}}^{\varepsilon_{max}} q\mathrm{d}\varepsilon \text{ (area under the loading curve)} \tag{13a}$$

$$E_{res} = \int_{\varepsilon_{max}}^{\varepsilon_{min}} q\mathrm{d}\varepsilon \text{ (area under the unloading curve)} \tag{13b}$$

368
369 Figure 13c shows the amount of dissipated energy during the last cycle before the rest period
370 (i.e. at plastic shakedown) and during the first cycle after the rest period. It is evident that for
371 the mixture with no rubber, the amount of energy dissipated is similar before and after the
372 rest period. When rubber is added, the mixture can dissipate a higher amount of energy after
373 each rest period. The greater the content of added rubber is, the higher the dissipated energy
374 and the corresponding efficiency ratio after each rest period (Fig. 13cd). Figure 13d also
375 shows that there is an increase in the energy dissipation efficiency by 35% after the rest
376 period for the mixture with RC = 15%. For a CWRC mixture, the total input energy is
377 dissipated in three main forms: (1) the sliding and rearrangement of particles, (2) the

deformation of particles and (3) the breakage of particles. As the rubber content increases (i.e. compressible component), more energy is dissipated through the compression and deformation of rubber particles and less energy is dissipated through densification and breakage. This is supported by the fact that more load cycles are needed to reach shakedown (a phenomenon associated with the rearrangement of particles) when the rubber content increases (Fig. 3d-f). When a rest period is introduced and the RC partially recover their volume, they also recover their energy dissipation potential that was gradually lost during cyclic densification, thus reducing particle degradation as less energy is dissipated through the breakage of particles.

DISCUSSION

Use as a Capping Material

To ensure an acceptable serviceability level, the maximum allowable axial deformation of a capping layer is 3 mm (Teixeira et al. 2006), corresponding to an axial strain of 2%. Figure 3a shows that for a confining pressure of 25 kPa and a cyclic deviator stress of 40 kPa the permanent axial strain after 200,000 cycles is less than 2% for all CWRC mixtures. The axial strain increases slightly when the confining pressure and the cyclic deviator stress increase to 50 kPa and 80 kPa respectively but remains less than 2% for up to 10% rubber content. This indicates that the mixture can be used in most rail corridors as a capping seam underneath the ballast layer, except for very heavy axle loads (e.g. iron ore freight rail). Under a relatively low confining pressure of 25 kPa and cyclic deviator stress of 100 kPa (CSR = 2.0), Fig. 3c shows that the axial strain increases to more than 2% after a few cycles when rubber is added. However, this excessive accumulation in axial strain is partly recovered when the load is removed. Therefore, this can be considered as an initial densification stage which in practice, will inevitably occur during construction and when placing and tamping the overlying ballast.

Figure 5a shows that the permanent axial strain after initial densification with respect to the new datum (dotted line) for all CWRC mixtures is less than 2%.

Figure 13c shows that the maximum energy dissipated after cyclic densification corresponds to RC = 10%, which means that a mixture with 10% RC has the highest capacity to dissipate energy after being subjected to a large number of dynamic loads from passing trains. Figure 13d also shows that the mixture with RC = 10% has the highest ER (efficiency ratio) after a rest period, after which there is only a marginal increase in ER for increased rubber content. Fig. 12 also shows that the BI of the mixture with RC > 5% decreases despite the increase in the number of cycles when a rest period is applied. This means that in practice, for a rubber content greater than 5% the mixture can recover a sufficient proportion of its energy dissipation efficiency during the rest period, thereby reducing breakage when subjected to a significantly high number of loading cycles (say N > 200,000). Therefore, based on the deformation response, energy dissipation and particle breakage, the mixture with 10% of added rubber can be justifiably recommended as an appropriate capping material for track substructure.

Environmental Impact and Sustainable Practices

Waste materials like CW and RC are much cheaper than traditional aggregates, making them more economical for the construction industry involved in the construction or maintenance of transportation corridors. Also, in some places where coal reject is stockpiled and good quality rock aggregates are not available, the reuse of CW minimizes the cost of transporting material from the source to the site. Therefore, the promising results presented in this study should create an incentive for the construction industry to start adopting more sustainable practices by using such waste materials in construction activities.

In Australia, the landfilling of CW is levied at $14 per ton, which is equivalent to spending millions of dollars per year on stockpiles of CW. Therefore, selling coal wash to the

427 construction industry instead of stockpiling it for a levy is a double win for the coal mining
428 industry. It gives them the chance to reverse part of the damage that coal mining causes to the
429 environment and it can solve some of the disputes over waste landfills between
430 environmentalists and the industry. In this context, it is in the interests of the coal mining
431 industry to consider, promote, and fund any initiative to reuse CW as a construction fill.
432 The rubber producing industry is no better than the coal mining industry when it comes to the
433 massive amounts of waste generated worldwide and the associated environmental risks. In
434 2016, 100,000 metric tons of discarded rubber caught fire in Madrid, Spain, causing several
435 thousand residents to be evacuated from their homes (Moffett 2016). The toxins emitted from
436 this fire can cause very serious health problems and possible land contamination when the
437 residues of burnt tyres infiltrate the soil with rain. Therefore, promoting the recycling of
438 rubber products such as waste rubber tyres is also an opportunity for the rubber producing
439 industry to reduce its carbon footprint and engage in sustainable practices.

440 **CONCLUSION**

441 The dynamic behaviour of the CWRC mixtures was investigated through a series of drained
442 cyclic triaxial tests with and without a rest period. Based on the experimental results, the
443 following conclusions can be drawn:

444 1. The permanent axial and volumetric strain increased with increasing rubber contents.
445 All the mixtures reached a plastic shakedown, but more load cycles were required to
446 attain a stable state when the rubber content increases. The permanent axial strain of
447 the mixtures measured before the rest period was higher than that measured after a
448 rest period. This shows that a rest period must be considered during cyclic loading
449 when investigating the resilient behaviour of a mixture with a compressible
450 component. No signs of frictional failure were detected for RC $\leq$ 15 % even for a
451 YCSR = 1.0 and a PCSR as high as 0.76.

2. For the mixtures with rubber, the total volumetric strain evaluated using local strain measurements was larger than the void volumetric strain. This indicates that during cyclic densification, the volume of RC cannot be considered as constant and the difference between the total volumetric strain and the void volumetric strain represents the associated change in the volume of the solid phase. Accordingly, a modified void ratio equation was derived to capture the deformation of rubber particles which can be applied to any mixture with a compressible component.
3. The resilient modulus and the shear modulus of the mixture decreased with increasing rubber contents, while the inclusion of RC improved the damping ratio of the mixture. When the CSR increased, the damping ratio of the mixture with no rubber decreased significantly whereas the mixtures with RC $\geq$ 5% maintained the same damping ratio. This shows that for higher stress levels, adding rubber preserves the damping potential of the mixture even after long periods of cyclic densification.
4. The BI of the mixture decreased significantly when rubber was added, and it decreased more for mixtures with RC $\geq$ 10% when a rest period was applied, despite the number of load cycles doubling. This shows that the efficiency of energy dissipation increases as the rubber content increases, and the energy dissipation potential can be partially recovered during a rest period, thus reducing particle breakage for longer periods of cyclic loading.
5. Based on the dynamic response in terms of axial deformation, efficiency in energy dissipation and reduction in particle breakage, the mixture with RC = 10% is recommended as the optimum blend for a capping material. From other practical perspectives, the reuse of the CWRC mixture as a construction fill is a sustainable environmental solution in relation to the quarrying of natural materials, and an economically attractive option for large scale landfilling and backfilling of spent coal

mines. In essence, recycling of these waste materials as an engineering fill is an immense contribution towards a favourable carbon footprint.

While promising results were presented in this study using conventional cyclic triaxial testing, it will be useful to test these type of mixtures in large-scale physical modelling to examine the role of a capping layer composed of this waste mixture on the response of a ballasted track section in terms of particle degradation and associated track deformation. Moreover, in contrast to drained behaviour, the fully undrained stress-strain response of saturated CW and rubber mixtures needs to be studied, because partially submerged track conditions often prevail in low-lying coastal terrains.

DATA AVAILABILITY STATEMENT

Some or all data, models, or code that support the findings of this study are available from the corresponding author upon reasonable request.

ACKNOWLEDGMENTS

The authors would like to thank the financial support from the Australian Research Council (ARC) Linkage Project (LP160100280) and Discovery Project (DP170101279). Financial and technical assistance provided by the industry partners of LP160100280, i.e. Ms. Robyn Lyster and Mr. Damian Mulcahy (RMS), Mr. Geoff McIntosh and Mr. Arthur Castrissios (Douglas Partners) and Mr. Michael Arroyo (South32) is gratefully acknowledged. The assistance provided by South32 in the procurement of CW material used in this study and the assistance provided by Richard Berndt in the performance of laboratory tests are also gratefully appreciated.

NOTATION

The following symbols are used in this paper

CW = coal wash

ER = efficiency ratio
RC = rubber crumbs
D = damping ratio
e = void ratio;
e_0 = initial void ratio;
G = shear modulus
M_r = resilient modulus
q_{cyc} = cyclic deviator stress;
q_{yield} = yield deviator stress under monotonic loading conditions;
q_{peak} = peak deviator stress under monotonic loading conditions;
V_v = volume of voids within specimen;
V_s = volume of solids within specimen;
V_{RC} = volume of rubber crumbs within specimen;
ε_1 = axial strain
ε_1^p = permanent axial strain;
ε_1^r = resilient axial strain (recoverable)
ε_3 = radial strain
ε_v = total volumetric strain;
ε_v^* = void volumetric strain
ε_v^s = solid volumetric strain
σ_3' = effective confining pressure;

500

501

REFERENCES

Ahmed, I. (1993). "Laboratory Study on Properties of Rubber-Soils." Joint Highway Research Project, Indiana Department of Transportation and Purdue University, West Lafayette, Indiana.

Chiaro, G., Indraratna, B., Tasalloti, S. A., and Rujikiatkamjorn, C. (2015). "Optimisation of coal wash-slag blend as a structural fill." *Proc., Institution of Civil Engineers: Ground Improvement*, 33-44.

Collins, I., Wang, A., and Saunders, L. (1993). "Shakedown theory and the design of unbound pavements." *Road and Transport Research*, 2(4), 28-39.

Feng, Z., and Sutter, K. (2000). "Dynamic Properties of Granulated Rubber/Sand Mixtures." *Geotechnical Testing Journal*, 23(3), 338-344.

Genever, M., O'Farrell, K., Randell, P., and Rebbechi, J. (2017). "National market development strategy for used tyres - Final Strategy."

Gu, F., Zhang, Y., Luo, X., Sahin, H., and Lytton, R. L. (2017). "Characterization and prediction of permanent deformation properties of unbound granular materials for Pavement ME Design." *Construction and Building Materials*, 155, 584-592.

Heitor, A., Indraratna, B., Kaliboullah, C. I., Rujikiatkamjorn, C., and McIntosh, G. W. (2016). "Drained and undrained shear behavior of compacted coal wash." *Journal of Geotechnical and Geoenvironmental Engineering*, 142(5), 04016006-04016001-04016006-04016010.

Indraratna, B. (1994). "Geotechnical characterization of blended coal tailings for construction and rehabilitation work." *Quarterly Journal of Engineering Geology*, 27, Part 4, 353-361.

Indraratna, B., Salim, W., and Rujikiatkamjorn, C. (2011). *Advanced Rail Geotechnology – Ballasted Track*, CRC Press, Leiden, Netherlands

Indraratna, B., Qi, Y., and Heitor, A. (2018). "Evaluating the Properties of Mixtures of Steel Furnace Slag, Coal Wash, and Rubber Crumbs Used as Subballast." *Journal of Materials in Civil Engineering*, 30(1), 04017251.

Indraratna, B., Qi, Y., Ngo, T.N., Rujikiatkamjorn, C., Neville, T., Ferreira, F.B. and Shahkolahi, A. (2019a). "Use of geogrids and recycled rubber in railroad infrastructure for enhanced performance-laboratory and computational study". Geosciences, 9(30).

Indraratna, B., Qi, Y., Tawk, M., Heitor, A., Rujikiatkamjorn, C. and Navaratnarajah, S.K. (2020). 'Advances in Ground Improvement Using Waste Materials for Transportation Infrastructure'. Ground Improvement, DOI: 10.1680/jgrim.20.00007.

Indraratna, B., Rujikiatkamjorn, C., Tawk, M., and Heitor, A. (2019b). "Compaction, degradation and deformation characteristics of an energy absorbing matrix." *Transportation Geotechnics*, 19, 74-83.

Lackenby, J., Indraratna, B., McDowell, G., and Christie, D. (2007). "Effect of confining pressure on ballast degradation and deformation under cyclic triaxial loading." *Geotechnique*, 57(6), 527-536.

Lee, J. H., Salgado, R., Bernal, A., and Lovell, C. W. (1999). "Shredded Tires and Rubber-Sand as Lightweight Backfill." *Journal of Geotechnical and Geoenvironmental Engineering*, 125(2), 132-141.

Lekarp, F., Isacsson, U., and Dawson, A. (2000a). "State of the Art I: Resilient Response of Unbound Aggregates." *Journal of Transportation Engineering*, 126(1), 66-75.

Lekarp, F., Isacsson, U., and Dawson, A. (2000b). "State of the Art II: Permanent Strain Response of Unbound Aggregates." *Journal of Transportation Engineering*, 126(1), 76-83

551 Leventhal, A. (1996)."Coal Washery Reject as an Engineered Material." *Proc., National*
552 *Symposium on the Use of Recycled Materials in Engineering Construction*, Institution
553 of Engineers, Australia, Barton, ACT, 54-59.
554 Leventhal, A., and De Ambrosis, L. (1985). "Waste disposal in coal mining—a geotechnical
555 analysis." *Engineering geology*, 22(1), 83-96.
556 Moffett, M. (2016). "Spanish Tire-Dump Blaze Sparks Health Alert: Several thousand
557 residents evacuated from homes near the fire." *The Wall Street Journal*.
558 https://www.wsj.com/articles/spanish-tire-dump-blaze-sparks-health-alert-
559 1463154848.
560 Montgomery, D. G. (1990)."Utilisation of Coal Washery Wastes in Engineering
561 Construction." *Proc., International Coal Engineering Conference*, Institution of
562 Engineers, Australia, 79-83.
563 Okagbue, C. O., and Ochulor, O. H. (2007). "The potential of cement-stabilized coal-reject as
564 a construction material." *Bulletin of Engineering Geology and the Environment*,
565 66(2), 143-151.
566 Qi, Y. and Indraratna, B. (2020). "Energy-based approach to assess the performance of a
567 granular matrix consisting of recycled rubber, steel furnace slag and coal wash".
568 *Journal of Materials in Civil Engineering*, 32(7), 04020169.
569 Qi, Y., Indraratna, B., Heitor, A., and Vinod, J. S. (2018a). "Effect of Rubber Crumbs on the
570 Cyclic Behavior of Steel Furnace Slag and Coal Wash Mixtures." *Journal of*
571 *Geotechnical and Geoenvironmental Engineering*, 144(2), 04017107.
572 Qi, Y., Indraratna, B. and Vinod, J.S. (2018b). "Behavior of Steel Furnace Slag, Coal Wash,
573 and Rubber Crumb Mixtures, with Special Relevance to Stress-dilatancy Relation".
574 *Journal of Materials in Civil Engineering*, ASCE, 30(11): 04018276.
575 Rujikiatkamjorn, C., Indraratna, B., and Chiaro, G. (2013). "Compaction of coal wash to
576 optimise its utilisation as water-front reclamation fill." *Geomechanics and*
577 *Geoengineering*, 8(1), 36-45.
578 Saberian, M., Li, J., Nguyen, B., and Wang, G. (2018). "Permanent deformation behaviour of
579 pavement base and subbase containing recycle concrete aggregate, coarse and fine
580 crumb rubber." *Construction and Building Materials*, 178, 51-58.
581 Saberian, M., Li, J., and Setunge, S. (2019). "Evaluation of permanent deformation of a new
582 pavement base and subbase containing unbound granular materials, crumb rubber and
583 crushed glass." *Journal of Cleaner Production*, 230, 38-45.
584 Senetakis, K., Anastasiadis, A., and Pitilakis, K. (2012). "Dynamic properties of dry
585 sand/rubber (SRM) and gravel/rubber (GRM) mixtures in a wide range of shearing
586 strain amplitudes." *Soil Dynamics and Earthquake Engineering*, 33(1), 38-53.
587 Signes, C. H., Fernández, P. M., Garzón-Roca, J., de la Torre, M. E. G., and Franco, R. I.
588 (2016). "An Evaluation of the Resilient Modulus and Permanent Deformation of
589 Unbound Mixtures of Granular Materials and Rubber Particles from Scrap Tyres to be
590 Used in Subballast Layers." *Transportation Research Procedia*, 18, 384-391.
591 Suiker, A. S. J., Selig, E. T., and Frenkel, R. (2005). "Static and Cyclic Triaxial Testing of
592 Ballast and Subballast." *Journal of Geotechnical and Geoenvironmental Engineering*,
593 131(6), 771-782.
594 Tasalloti, S. A., Indraratna, B., Rujikiatkamjorn, C., Heitor, A., and Chiaro, G. (2015). "A
595 laboratory study on the shear behavior of mixtures of coal wash and steel furnace slag
596 as potential structural fill." *Geotechnical Testing Journal*, 38(4), 361-372.
597 Tawk, M. and Indraratna, B. (2020). “Role of Rubber Crumbs on the Stress-Strain Response
598 of a Coal Wash Matrix.” *Journal of Materials in Civil Engineering*. DOI:
599 10.1061/(ASCE)MT.1943-5533.0003514

Teixeira, P. F., López-Pita, A., Casas, C., Bachiller, A., and Robusté, F. (2006). "Improvements in High-Speed Ballasted Track Design:Benefits of Bituminous Subballast Layers." *Transportation Research Record*, 1943(1), 43-49.

U.S. Tire Manufacturers Association (2018). "2018 USTMA Sustainability Progress Report." https://www.ustires.org/sustainability-report.

Wang, D., Tawk, M., Indraratna, B., Heitor, A., and Rujikiatkamjorn, C. (2019). "A mixture of coal wash and fly ash as a pavement substructure material." *Transportation Geotechnics*, 21, 100265.

Werkmeister, S., Dawson, A. R., and Wellner, F. (2001). "Permanent Deformation Behavior of Granular Materials and the Shakedown Concept." *Transportation Research Record*, 1757(1), 75-81.

Youwai, S., and Bergado, D. T. (2003). "Strength and deformation characteristics of shredded rubber tire-sand mixtures." *Canadian Geotechnical Journal*, 40(2), 254-264.

614 **List of Tables**

615 **Table 1.** Properties of the cyclic triaxial tests

616

Table 1. Properties of the cyclic triaxial tests

Test #	Added rubber (%)	σ'_3 (kPa)	q_{cyclic} (kPa)	CSR	YCSR	PCSR
C1	0	25	40	0.8	0.43	0.19
C2	5			0.8	0.38	0.21
C3	10			0.8	0.42	0.26
C4	15			0.8	0.43	0.30
C5	0	50	80	0.8	0.39	0.24
C6	5			0.8	0.43	0.27
C7	10			0.8	0.43	0.29
C8	15			0.8	0.46	0.35
C9	0	25	100	2.0	1.08	0.47
C10	5			2.0	0.96	0.54
C11	10			2.0	1.04	0.65
C12	15			2.0	1.07	0.76
C13*	0	25	100	2.0	1.08	0.47
C14*	5			2.0	0.96	0.54
C15*	10			2.0	1.04	0.65
C16*	15			2.0	1.07	0.76

*Cyclic triaxial tests with a rest period; CSR = cyclic stress ratio; YCSR = yield cyclic stress ratio; PCSR = peak cyclic stress ratio.

List of Figures

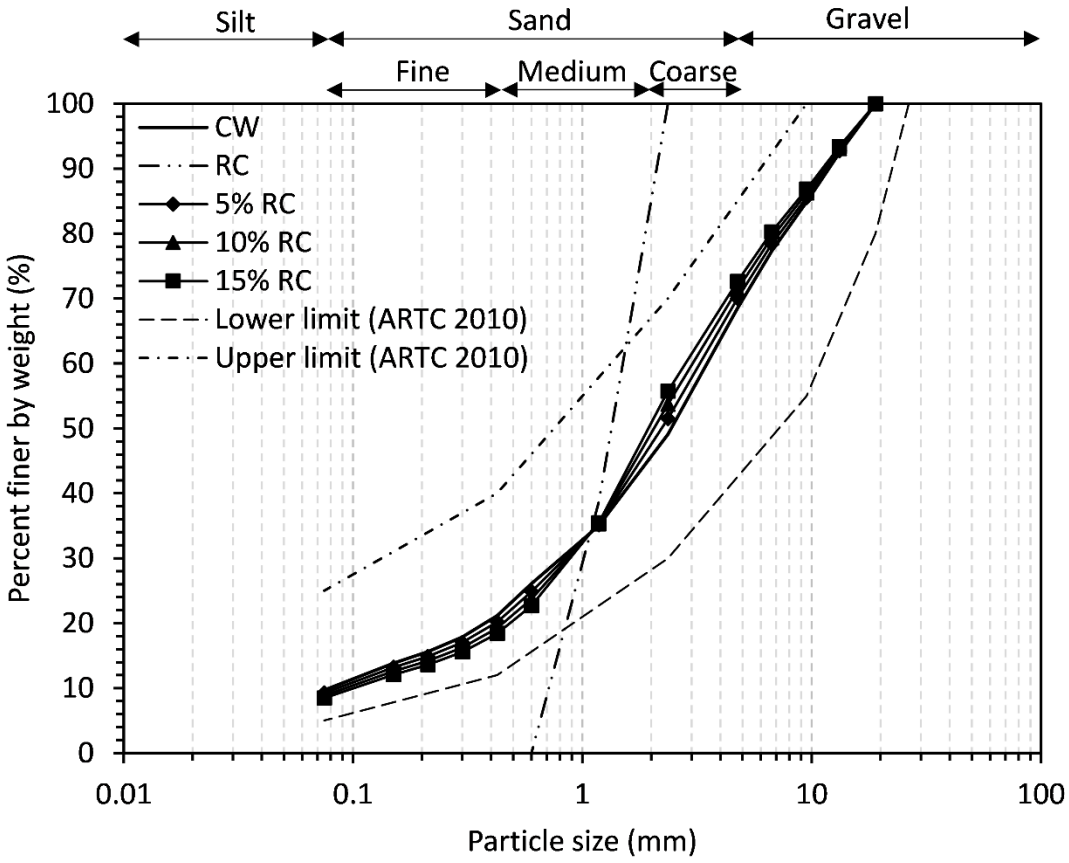

653

654 **Figure 1** PSD curves of CW, RC, and CWRC mixtures.

655

656

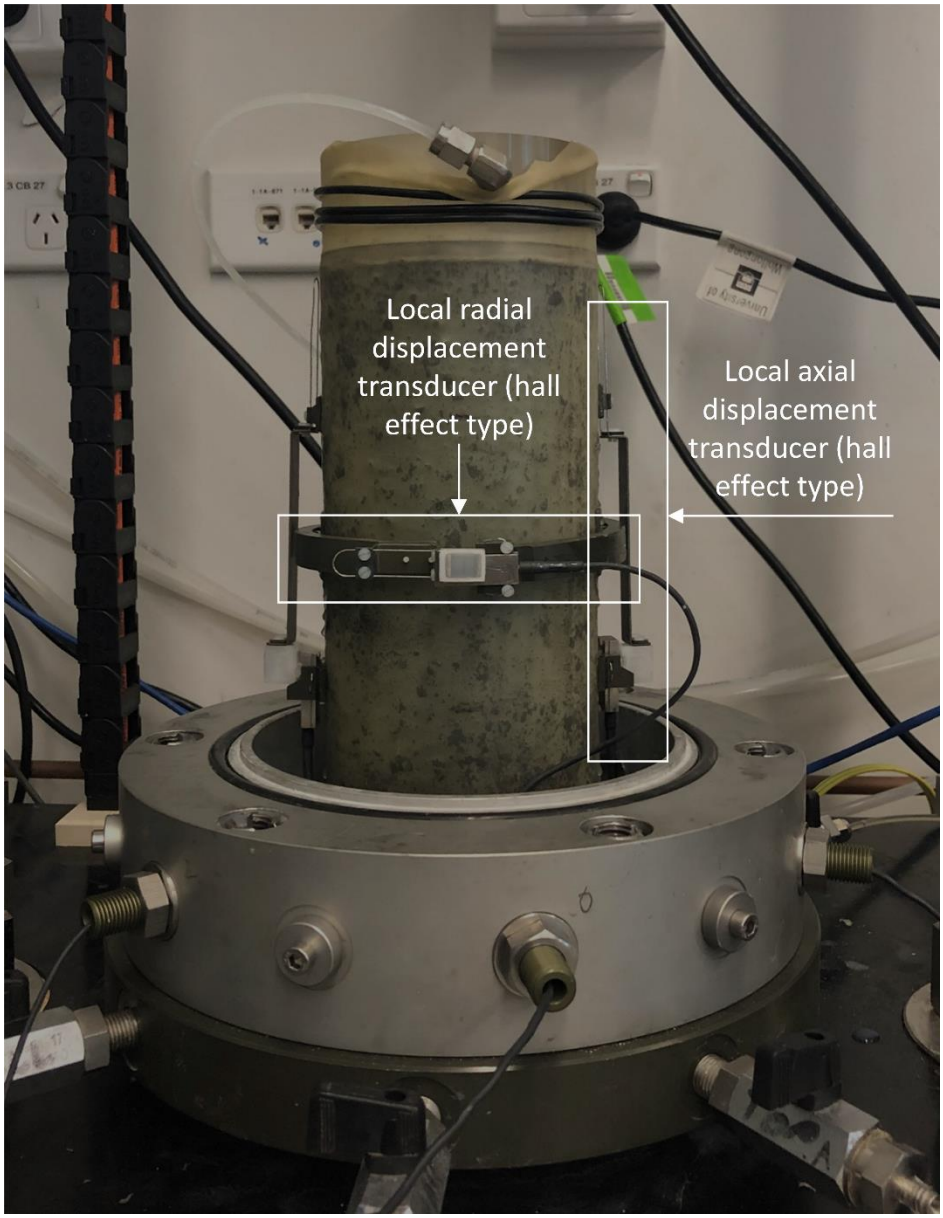

Figure 2 Sample mounted with hall effect sensors for local strain measurement.

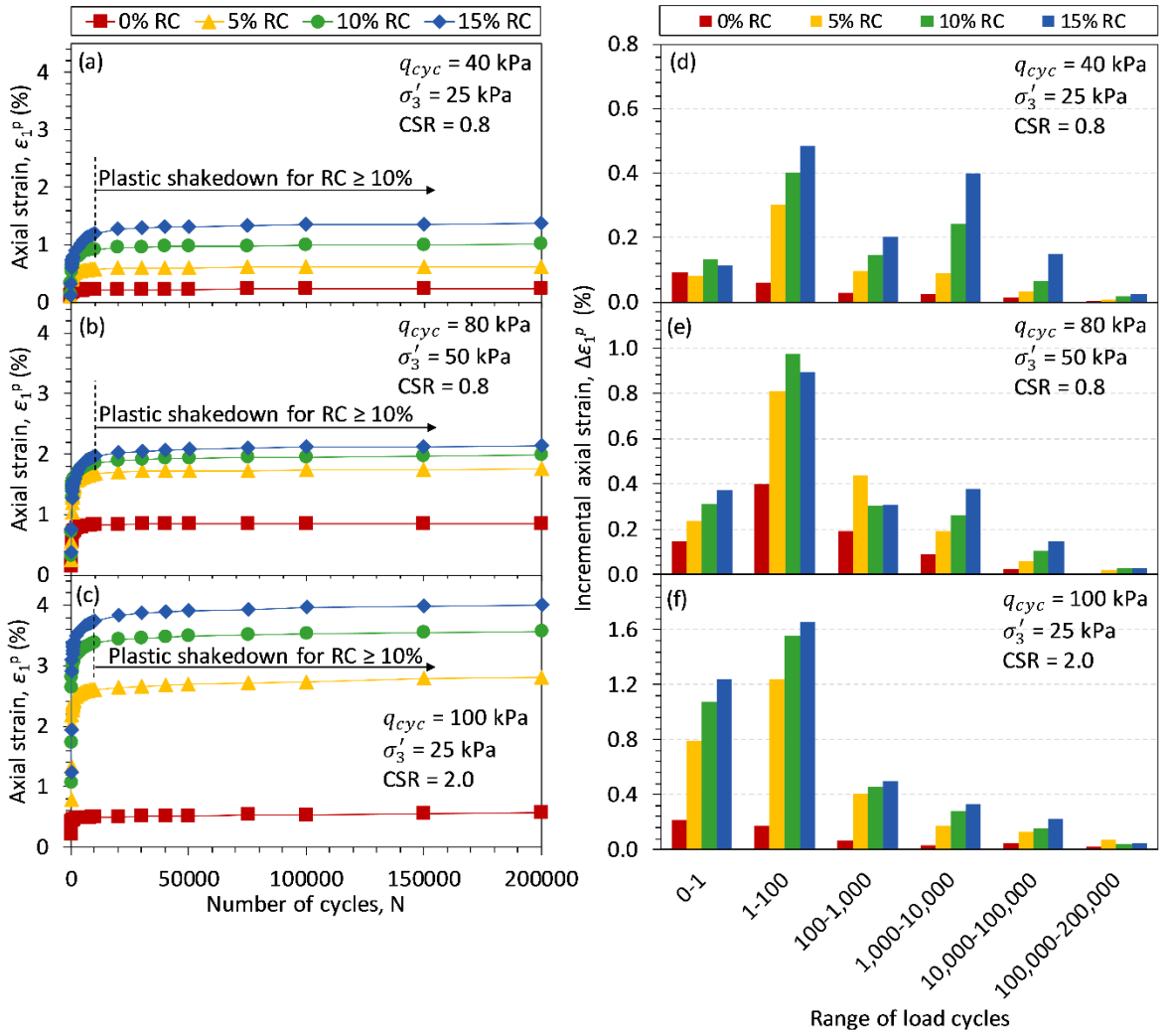

Figure 3 Permanent axial strain for (a) σ_3' = 25 kPa and q_{cyc} = 40 kPa, (b) σ_3' = 50 kPa and q_{cyc} = 80 kPa and (c) σ_3' = 25 kPa and q_{cyc} = 100 kPa and incremental axial strain for (d) σ_3' = 25 kPa and q_{cyc} = 40 kPa, (e) σ_3' = 50 kPa and q_{cyc} = 80 kPa and (f) σ_3' = 25 kPa and q_{cyc} = 100 kPa

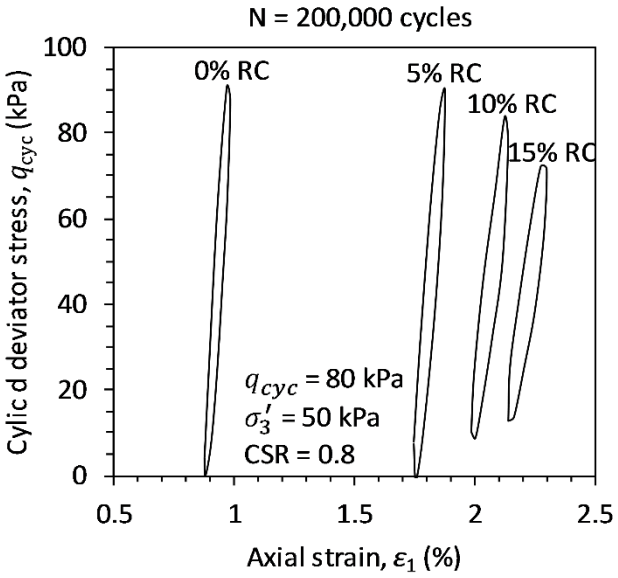

668

669 **Figure 4.** Stress-strain loop after 200,000 cycles for σ_3' = 50 kPa and q_{cyc} = 80 kPa.

670

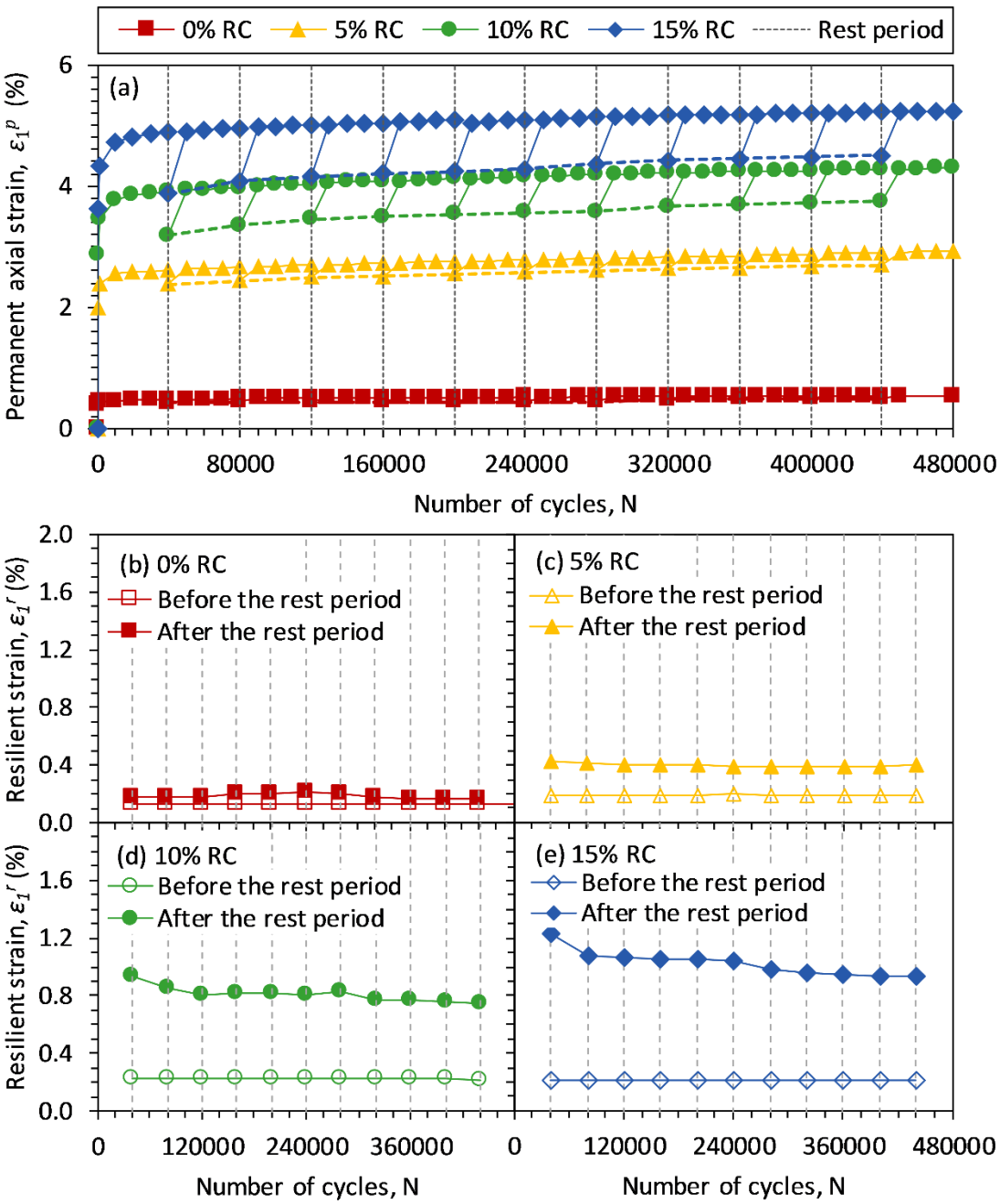

671

672 **Figure 5.** Effect of applying a rest period on (a) the permanent axial strain of all CWRC
673 mixtures and the resilient strain of the CWRC mixture with (b) RC = 0%, (c) RC = 5%, (d)
674 RC = 10% and (e) RC = 15%.

675

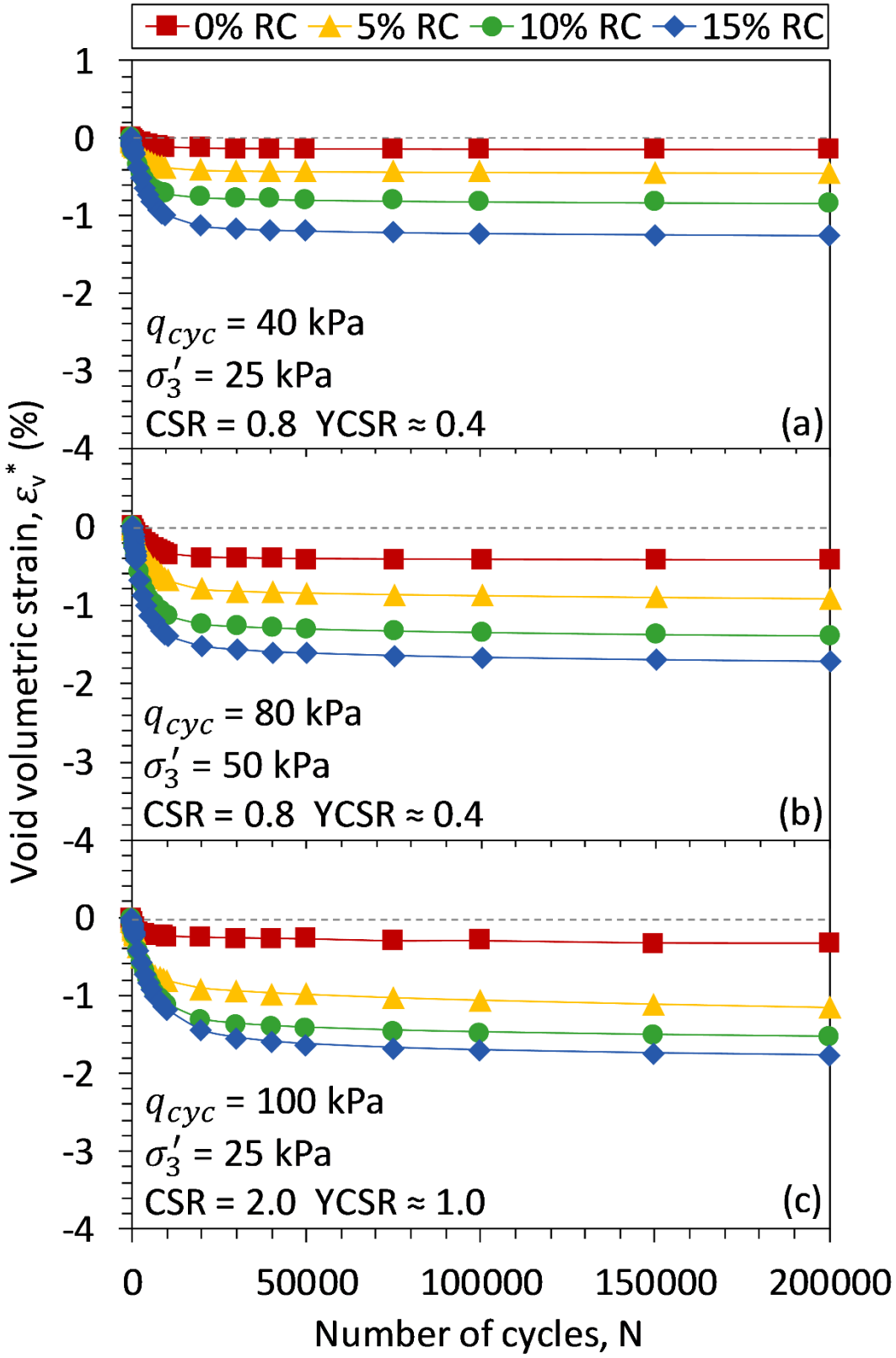

Figure 6. Void volumetric strain of CWRC mixtures for (a) σ_3' = 25 kPa and q_{cyc} = 40 kPa, (b) σ_3' = 50 kPa and q_{cyc} = 80 kPa and (c) σ_3' = 25 kPa and q_{cyc} = 100 kPa.

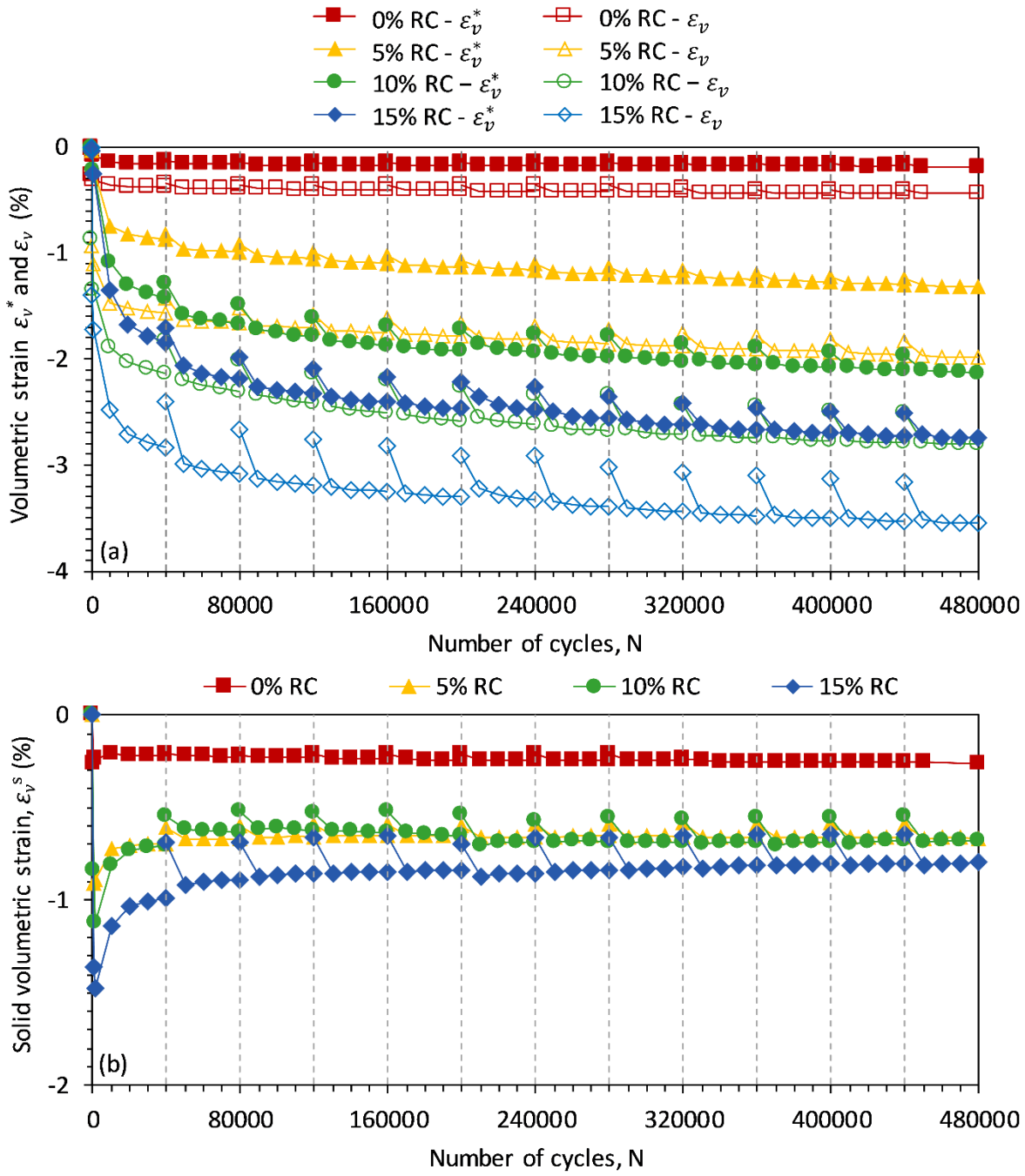

681

682 **Figure 7.** (a) Void volumetric strain, total volumetric strain and (b) solid volumetric strain of
683 CWRC mixtures with a rest period.

684

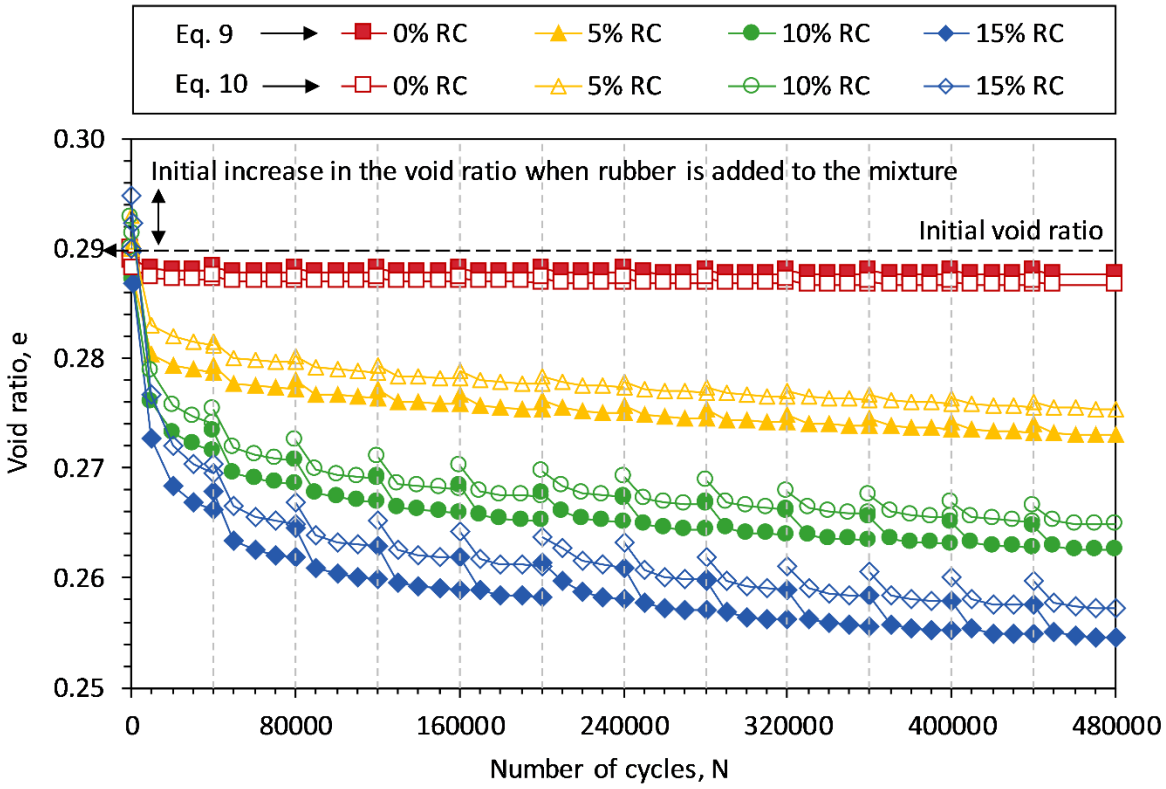

685

686 **Figure 8.** Effect of the change in the volume of RC on the void ratio as calculated by Eq. 9
687 and Eq. 10.

688

689

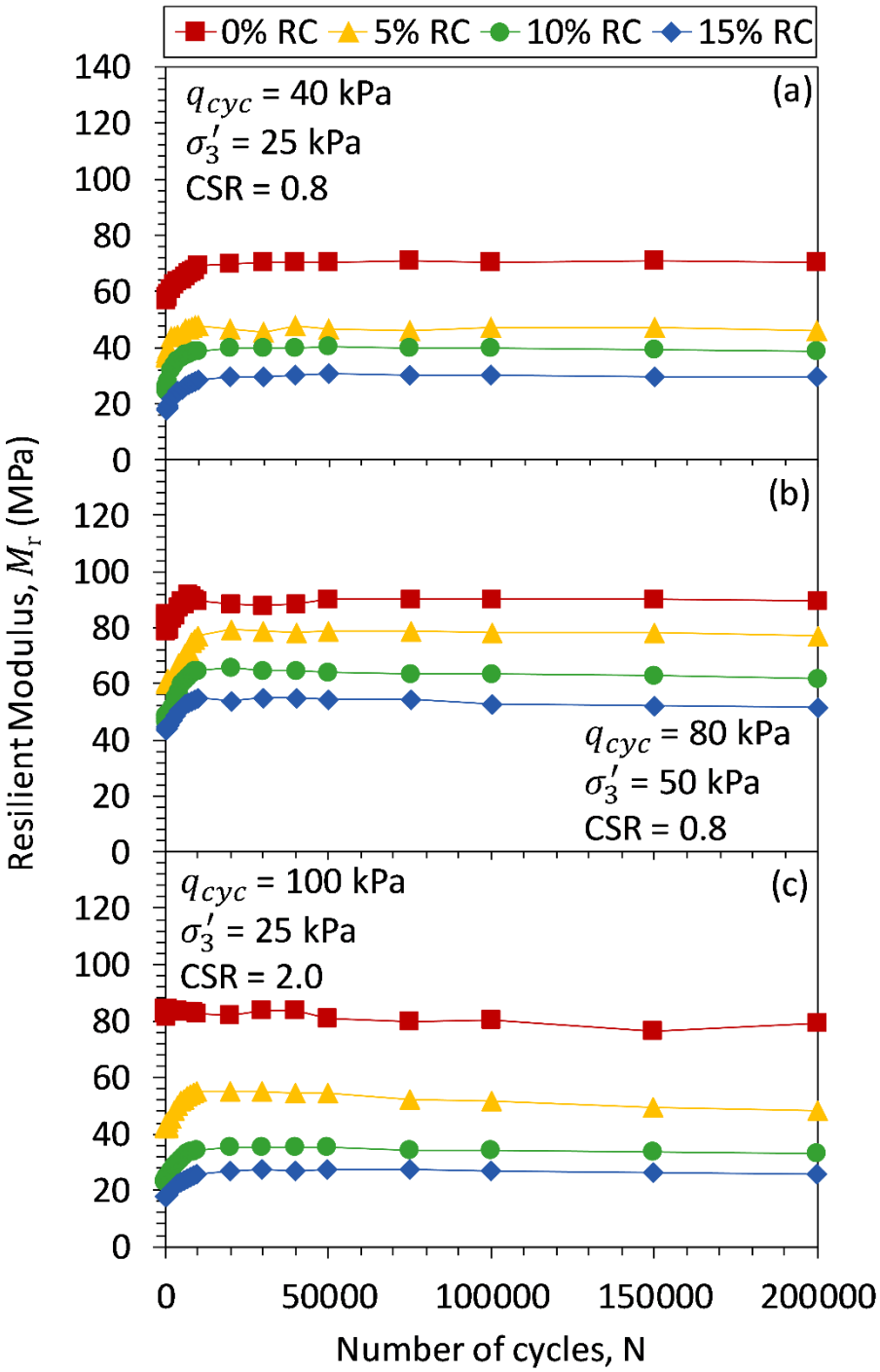

690

691 **Figure 9** Resilient modulus vs. number of cycles of CWRC mixtures for (a) σ_3' = 25 kPa and
692 q_{cyc} = 40 kPa, (b) σ_3' = 50 kPa and q_{cyc} = 80 kPa and (c) σ_3' = 25 kPa and q_{cyc} = 100 kPa.

693

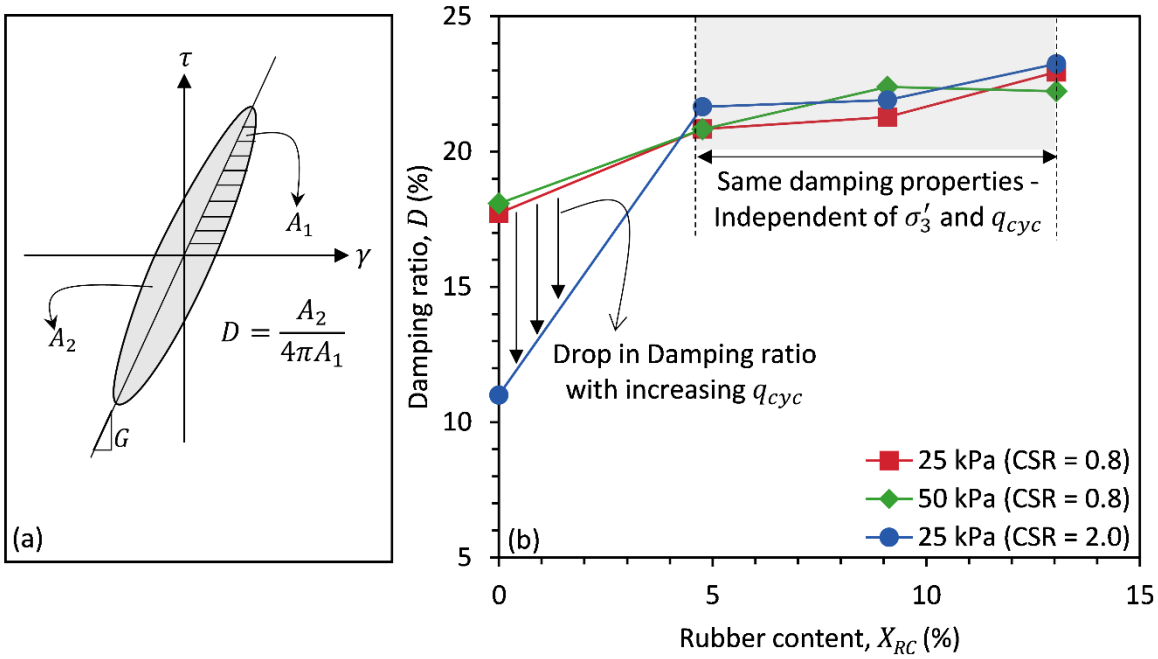

694

695 **Figure 10** (a) Definition of the damping ratio and the shear modulus and (b) damping ratio of
696 CWRC mixtures.

697

698

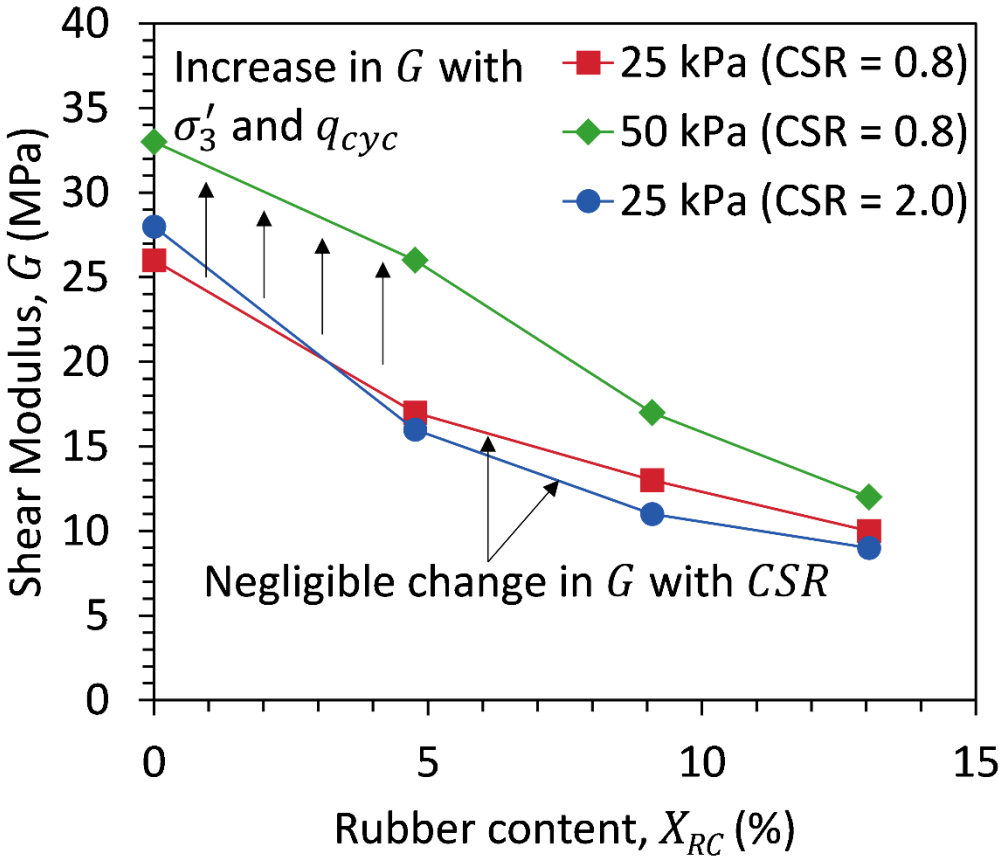

699

700 **Figure 11** Shear modulus of CWRC mixtures.

701

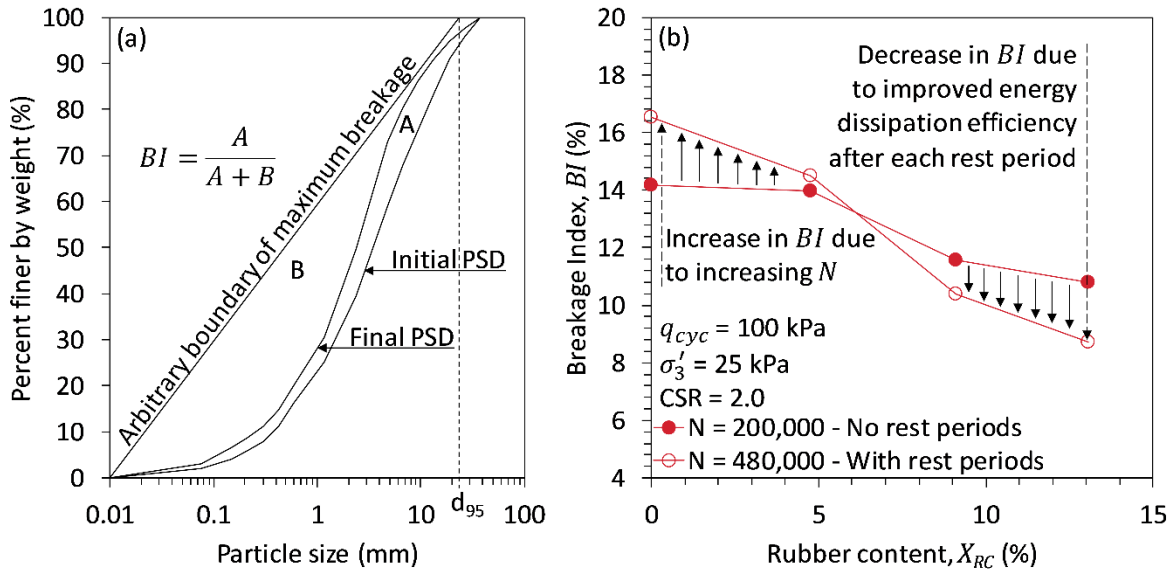

Figure 12. (a) Definition of the Breakage Index (BI) as proposed by Indraratna el al. (2005) and (b) the BI of the CWRC mixture with and without a rest period.

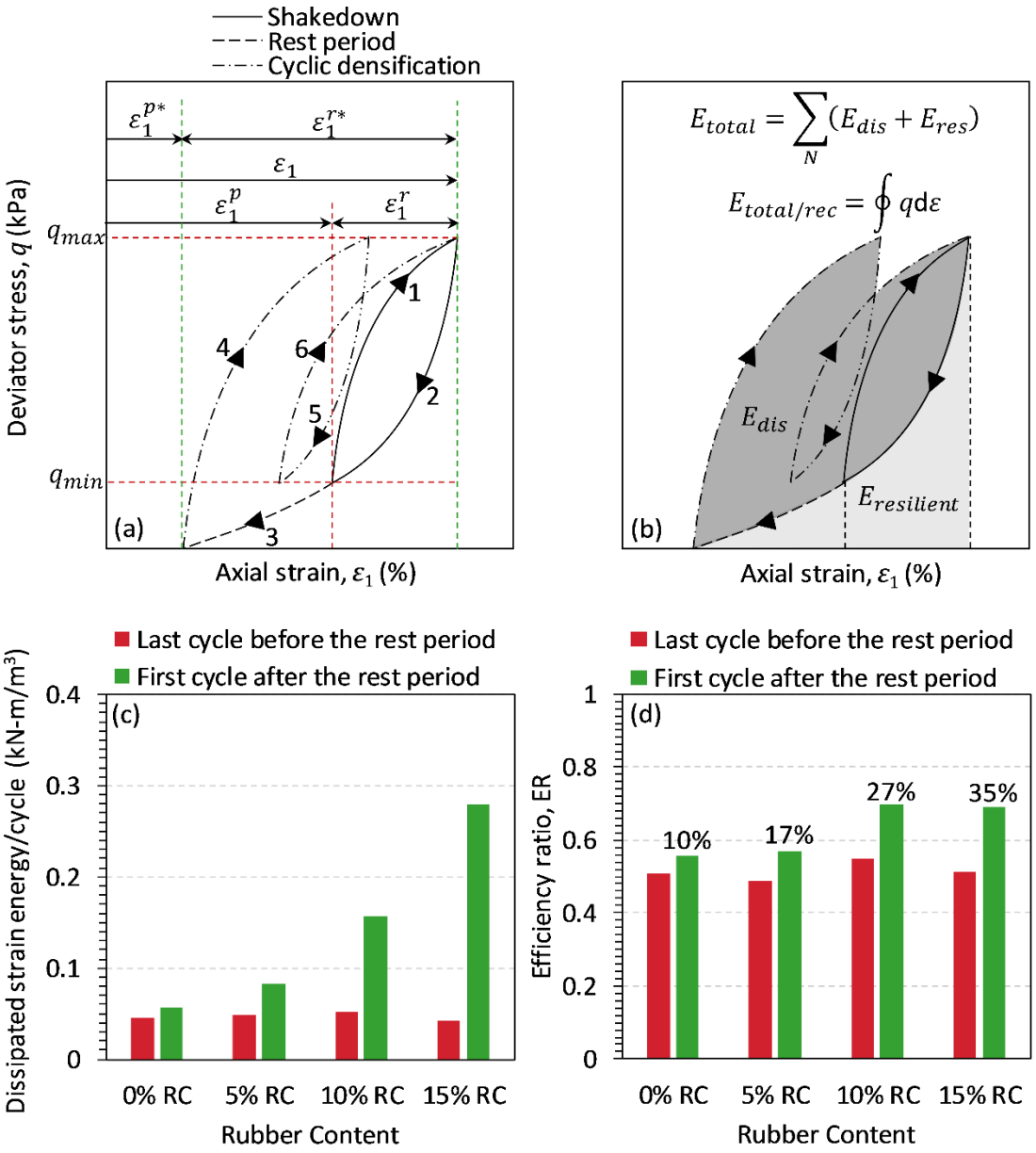

Figure 13. (a) Evolution of the stress strain loop during cyclic densification, shakedown and the rest period, (b) definition of dissipated energy during cyclic loading, (c) dissipated strain energy/cycle of CWRC mixtures and (d) efficiency ratio (ER) of CWRC mixtures.